*Original Article*

# The Role of $Ca^{2+}$ Influx for Insulin-Mediated Glucose Uptake in Skeletal Muscle

**Johanna T. Lanner,[1] Abram Katz,[1] Pasi Tavi,[2] Marie E. Sandström,[1] Shi-Jin Zhang,[1] Charlott Wretman,[3] Stephen James,[3] Jérémy Fauconnier,[1] Jan Lännergren,[1] Joseph D. Bruton,[1] and Håkan Westerblad[1]**

**The involvement of $Ca^{2+}$ in insulin-mediated glucose uptake is uncertain. We measured $Ca^{2+}$ influx (as $Mn^{2+}$ quenching or $Ba^{2+}$ influx) and 2-deoxyglucose (2-DG) uptake in single muscle fibers isolated from limbs of adult mice; 2-DG uptake was also measured in isolated whole muscles. Exposure to insulin increased the $Ca^{2+}$ influx in single muscle cells. $Ca^{2+}$ influx in the presence of insulin was decreased by 2-aminoethoxydiphenyl borate (2-APB) and increased by the membrane-permeable diacylglycerol analog 1-oleyl-2-acetyl-*sn*-glycerol (OAG), agents frequently used to block and activate, respectively, nonselective cation channels. Maneuvers that decreased $Ca^{2+}$ influx in the presence of insulin also decreased 2-DG uptake, whereas increased $Ca^{2+}$ influx was associated with increased insulin-mediated glucose uptake in isolated single cells and whole muscles from both normal and insulin-resistant obese *ob/ob* mice. 2-APB and OAG affected neither basal nor hypoxia- or contraction-mediated 2-DG uptake. 2-APB did not inhibit the insulin-mediated activation of protein kinase B or extracellular signal–related kinase 1/2 in whole muscles. In conclusion, alterations in $Ca^{2+}$ influx specifically modulate insulin-mediated glucose uptake in both normal and insulin-resistant skeletal muscle. Moreover, the present results indicate that $Ca^{2+}$ acts late in the insulin signaling pathway, for instance, in the GLUT4 translocation to the plasma membrane. *Diabetes* 55:2077–2083, 2006**

Skeletal muscle accounts for up to 50% of body weight and is the major site of insulin-mediated glucose disposal in humans (1). Insulin, via an incompletely understood cascade of reactions, stimulates the translocation of GLUT4 transport proteins from an intracellular site to the plasma membrane, where entry of glucose is facilitated (2–4). Knowledge of the complete sequence of steps in insulin signaling is crucial for devising strategies to cure or treat diseases associated with defects in insulin-mediated glucose disposal, such as type 2 diabetes.

Earlier research implicated a role of $Ca^{2+}$ in insulin-mediated activation of glucose transport in muscle (5–8). However, this idea did not achieve widespread acceptance, and recent reviews generally do not mention $Ca^{2+}$ in the insulin signaling cascade (2–4). One reason for excluding $Ca^{2+}$ is that the insulin-mediated glucose uptake was not decreased when skeletal muscles were bathed in a solution without added $Ca^{2+}$ (9,10). Furthermore, insulin did not increase cytosolic $[Ca^{2+}]$ in various tissues (11–13). In line with this, previous studies from our laboratory showed no effect of insulin on the global free myoplasmic $[Ca^{2+}]$ ($[Ca^{2+}]_i$) in isolated, intact rodent skeletal muscle fibers (14,15). However, insulin application resulted in a significant increase in $[Ca^{2+}]$ close to the cell membrane ($[Ca^{2+}]_{mem}$) in skeletal muscle fibers, and the insulin concentration required for half-maximal increase in $[Ca^{2+}]_{mem}$ was similar to that needed for half-maximal activation of insulin-mediated glucose uptake (14,15). The increase in $[Ca^{2+}]_{mem}$ was the result of $Ca^{2+}$ influx into the muscle cells because it was inhibited when extracellular $[Ca^{2+}]$ was decreased to the low nanomolar range (14).

In the present study, we hypothesized that $Ca^{2+}$ influx is important for insulin-mediated glucose uptake. We measured insulin-mediated $Ca^{2+}$ influx in the presence of pharmacological agents that are frequently used to manipulate $Ca^{2+}$ influx through nonselective cation channels: 2-aminoethoxydiphenyl borate (2-APB), which inhibits $Ca^{2+}$ influx (16–18), and the membrane-permeable, nonmetabolizable diacylglycerol analog 1-oleyl-2-acetyl-*sn*-glycerol (OAG), which stimulates $Ca^{2+}$ influx (19). The results show that decreases and increases in $Ca^{2+}$ influx were accompanied by corresponding changes in insulin-mediated glucose uptake.

## RESEARCH DESIGN AND METHODS

Adult male mice (NMRI or C57BL/6, weight ~30 g) or rats (Wistar, weight ~100 g) were housed at room temperature and fed ad libitum. In some experiments, male obese leptin-deficient *ob/ob* mice (45–55 g) were used. Animals were killed by rapid neck disarticulation and muscles removed. Isolated extensor digitorum longus (EDL; mainly fast-twitch fibers), flexor digitorum brevis (FDB; mainly fast-twitch fibers), and soleus (mainly slow-twitch fibers) muscles were used for measurements of 2-deoxyglucose (2-DG) uptake and protein phosphorylation. Intact single FDB fibers were used in experiments with fluorescent indicators measuring $Ca^{2+}$ influx and 2-DG uptake. The single fibers were obtained either by microdissection (20) or by

From the [1]Department of Physiology and Pharmacology, Karolinska Institutet, Stockholm, Sweden; the [2]Department of Physiology and Biocenter Oulu, University of Oulu, Oulun Yliopisto, Finland; and [3]Biovitrum, Stockholm, Sweden.

Address correspondence and reprint requests to Håkan Westerblad, Department of Physiology and Pharmacology, Karolinska Institutet, SE-171 77, Stockholm, Sweden. E-mail: hakan.westerblad@ki.se.

Received for publication 14 December 2005 and accepted in revised form 6 April 2006.

A.K. and H.W. have received research grants from Biovitrum.

2-APB, 2-aminoethoxydiphenyl borate; 2-DG, 2-deoxyglucose; 2-NBDG, 2-(*N*-[7-nitrobenz-2-oxa-1,3-diazol-4-yl]amino)-2-deoxyglucose; $[Ca^{2+}]_i$, intracellular calcium concentration; $[Ca^{2+}]_{mem}$, calcium concentration close to cell membrane; EDL, extensor digitorum longus; ERK, extracellular signal–related kinase; FDB, flexor digitorum brevis; MDL, *cis-N*-(2-phenylcyclopentyl)azacyclotridec-1-en-2-amine; OAG, 1-oleyl-2-acetyl-*sn*-glycerol; PKB, protein kinase B.

DOI: 10.2337/db05-1613

enzymatic digestion (21). All experiments on living cells were performed in solutions bubbled with 95% $O_2$/5% $CO_2$, with the exception of hypoxia experiments (see below). When used, insulin was applied at a supramaximal concentration of 60 or 120 nmol/l (10 or 20 mU/ml). All experiments were approved by the Stockholm North local ethical committee.

**$Ca^{2+}$ influx.** We used two highly sensitive methods to measure $Ca^{2+}$ influx that have been frequently used to study nonselective cation channel activity: $Mn^{2+}$ quenching (22) and $Ba^{2+}$ influx (17). In $Mn^{2+}$-quenching experiments, single FDB fibers were isolated by microdissection and mounted in a stimulation chamber continuously superfused by standard Tyrode solution (no glucose) (20). The fiber was microinjected with the fluorescent $Ca^{2+}$ indicator fura-2 (Invitrogen) and then excited at 360 ± 5 nm (the isosbestic wavelength of fura-2 under our experimental conditions), while measuring the fluorescence light emitted at 495 ± 5 nm. $MnCl_2$ (100 μmol/l) was first added to the bath solution to obtain the rate of basal quenching. We then applied insulin and/or 2-APB. The rate of $Mn^{2+}$ quenching was measured during periods where the rate of decrease of the fluorescent light was stable (i.e., ignoring transient changes induced by changes of the bath solution). Measurements were not performed until 2 min after application of insulin, thus allowing time for insulin to act. A brief tetanic contraction was produced before and after the period of exposures to ensure that the fiber was fully viable; fibers that showed a marked decrease (>10%) in tetanic force were discarded.

For $Ba^{2+}$ influx experiments, FDB fibers were enzymatically isolated and cultured for ≥20 h (21). The fibers were loaded with Calcium Green-1 (10 μmol/l; Invitrogen) for 1 h at room temperature. For imaging, we used a BioRad MRC 1024 confocal unit with a krypton/argon mixed-gas laser run at 15 mW (BioRad Microscopy Division, Hertfordshire, U.K.) attached to a Nikon Diaphot 200 inverted microscope. A Nikon Plan Apo 20× objective lens was used. The cells were excited at 488 nm, and the emitted light was collected through a 522-nm narrow-band filter simultaneously from six to eight cells at 10-s intervals. To measure the baseline fluorescence, cells were first superfused with normal, glucose-free Tyrode solution for 5 min. Cells were then exposed to the $Ba^{2+}$ solution, where 1 mmol/l $Ca^{2+}$ was replaced by 1 mmol/l $Ba^{2+}$, for 20 min. Data were normalized to the Calcium Green-1 fluorescence at the onset of $Ba^{2+}$ exposure, which was set to 1.0. When used, insulin, OAG, and/or 2-APB were added to the $Ba^{2+}$ solution. In a subset of experiments, cells were first exposed to insulin for 20 min, and OAG was then applied in the continued presence of insulin. Viability of the cells was tested before and after $Ba^{2+}$ experiments with brief electrical stimulation. We only used data from cells that contracted and displayed normal $[Ca^{2+}]_i$ transients in response to stimulation.

**Glucose uptake in single FDB fibers.** 2-(*N*-[7-nitrobenz-2-oxa-1,3-diazol-4-yl]amino)-2-deoxyglucose (2-NBDG; Invitrogen) has been used to assess glucose uptake in single vascular smooth muscle cells (23), and we adapted this method to single FDB fibers. Enzymatically digested FDB cells were cultured for ~20 h and then imaged using a BioRad MRC 1024 confocal microscope (see above) with illumination at 488 nm, while measuring the emitted light at >515 nm. Fibers were superfused with a glucose-free (2 mmol/l pyruvate) Tyrode solution containing 50 μmol/l 2-NBDG for 15 min and then washed for 20 min. Fibers were then again exposed to 50 μmol/l 2-NBDG for 15 min followed by 20 min of washing. When used, insulin, 2-APB, and/or OAG were present during the last 15 min of the first washing period and during the second exposure to 2-NBDG. In some experiments, the $[Ca^{2+}]$ in the Tyrode solution was decreased to ~1 nmol/l by decreasing the added $CaCl_2$ to 10 μmol/l, increasing $MgCl_2$ to 4.5 mmol/l, and adding 2 mmol/l EGTA. Up to six fibers were followed in each experiment, and only fibers that at the end of the experiment gave a robust contraction in response to electrical stimulation were included. Three confocal images were used to assess 2-NBDG uptake: immediately before the first exposure to 2-NBDG (a), after the first washing period (b), and after the second washing period (c). For each muscle fiber, the increase in fluorescence during the second 2-NBDG exposure period ($\Delta F_{c-b}$) was divided by the increase in fluorescence during the first exposure ($\Delta F_{b-a}$). In each set of experiments, the mean $\Delta F_{c-b}/\Delta F_{b-a}$ of fibers in one dish, with insulin added on its own, was set to 100% and compared with the $\Delta F_{c-b}/\Delta F_{b-a}$ of fibers not exposed to insulin (basal), exposed to insulin in low $[Ca^{2+}]$, or exposed to insulin plus 2-APB or OAG.

**Glucose uptake in isolated whole muscles.** 2-DG uptake in whole muscles was measured essentially as described elsewhere (24). Briefly, muscles were incubated at 35°C in a shaking water bath in Krebs bicarbonate buffer containing 2 mmol/l pyruvate (no glucose) with or without OAG or an inhibitor of $Ca^{2+}$ influx, either 2-APB or *cis*-*N*-(2-phenylcyclopentyl)azacyclotridec-1-en-2-amine (MDL) (25). When used, insulin was applied 30 min before addition of 2-DG (1 mmol/l; 1 mCi per mmol/l) and inulin (1 μCi/ml medium). Muscles were blotted and frozen in liquid nitrogen 20 min after addition of 2-DG. Muscles were then weighed, digested in NaOH at 70°C, cooled, and centrifuged, and aliquots of the supernatants were added to scintillation cocktail and counted for $^3H$ (2-DG) and $^{14}C$ (inulin).

Hypoxia-mediated 2-DG uptake with or without 2-APB or OAG was studied by exposing muscles to 95% $N_2$/5% $CO_2$, instead of the normal 95% $O_2$/5% $CO_2$, for 80 min with 2-DG present during the last 20 min. The effect of 2-APB or OAG on contraction-mediated 2-DG uptake was studied in EDL muscles. The muscles were stimulated in standard Tyrode solution with two tetanic contractions (50 Hz, 100 ms) per second for 10 min, which results in a decrease in the glycogen store to <20% of the rested value (26). Muscles were transferred to the shaking water bath immediately after the cessation of tetanic contractions and incubated for 40 min with or without 100 μmol/l 2-APB or 30 μmol/l OAG. 2-DG uptake was measured during the last 20 min.

**Phosphorylation of protein kinase B and extracellular signal–related kinase 1/2.** For protein kinase B analyses, whole EDL muscles were incubated at 37°C in standard Tyrode solution with or without insulin, 2-APB, or wortmannin and then frozen in liquid nitrogen. Frozen muscles were homogenized in lysis buffer consisting of (in mmol/l): 20 Hepes (pH 7.6), 150 NaCl, 5 EDTA, 25 KF, and 1 $Na_3VO_4$, as well as protease inhibitor cocktail (Roche), 20% glycerol, and 0.5% Triton X-100. Lysates were cleared by centrifugation for 5 min at 1,000*g*. The protein content was determined using the Bradford assay (Bio-Rad). Phosphorylated protein kinase B (PKB) and total PKB were measured using the PathScan Elisa Kit (Cell Signaling 7160 and 7170, respectively) following the supplier's test procedures.

The phosphorylation state of the mitogen-activated protein kinase extracellular signal–related kinase (ERK) 1/2 was measured with Western blot and phospho-specific antibodies (New England Biolabs) as described elsewhere (27).

**Statistics.** Data are presented as means ± SE. Statistical analyses of two groups were performed as paired or unpaired *t* tests, as appropriate. We used one-way ANOVA for analyses of more than two groups and one-way repeated-measures ANOVA for repeated measurements in one group. When ANOVA yielded a significant difference, either the Student-Newman-Keuls or Dunnett's post hoc tests were used. *P* values <0.05 were considered statistically significant.

## RESULTS

**Effects of 2-APB on insulin- and OAG-induced $Ca^{2+}$ influx.** We used two methods frequently employed to detect $Ca^{2+}$ fluxes over the cell membrane: $Mn^{2+}$-quenching of fura-2 fluorescence (22) and $Ba^{2+}$ influx measured with the visible-light $Ca^{2+}$ indicator Calcium Green-1 (17). A major attraction with these methods is that they are very sensitive and can detect even small changes in the $Ca^{2+}$ influx.

The basal rate of $Mn^{2+}$ quenching was 0.70 ± 0.06%/min ($n$ = 11). Figure 1*A* shows a representative $Mn^{2+}$ quenching experiment with application of insulin followed by 2-APB. Insulin increased the rate of quenching in four of five cells tested (Fig. 1*B*). The subsequent application of 2-APB (100 μmol/l) resulted in a significant reduction of the rate of quenching ($P < 0.01$). Surprisingly, removal of 2-APB in the continued presence of insulin gave a rebound effect with a rate of quenching that was ~30% higher than basal ($P < 0.01$).

Application of insulin caused a significant increase in the $Ba^{2+}$ influx ($P < 0.001$) (Fig. 1*C* and *D*). Application of insulin and 2-APB caused a transient increase in the $Ba^{2+}$ influx, but at the end of the 20-min incubation period, the relative fluorescence was significantly lower than with insulin alone (Fig. 1*D*).

Application of OAG (30 μmol/l) caused a significant increase ($P < 0.001$) in the $Ba^{2+}$ influx with a magnitude similar to that obtained with insulin (Fig. 1*C*). However, the rate of increase was markedly lower with OAG than with insulin; the time to reach half the maximum signal was ~12 and 6 min, respectively. Application of OAG plus 2-APB caused a transient increase in the relative fluorescence (as was the case with insulin plus 2-APB), but at the end of the incubation period, the OAG-induced increase in $Ba^{2+}$ influx was abolished in the presence of 2-APB (Fig. 1*D*).

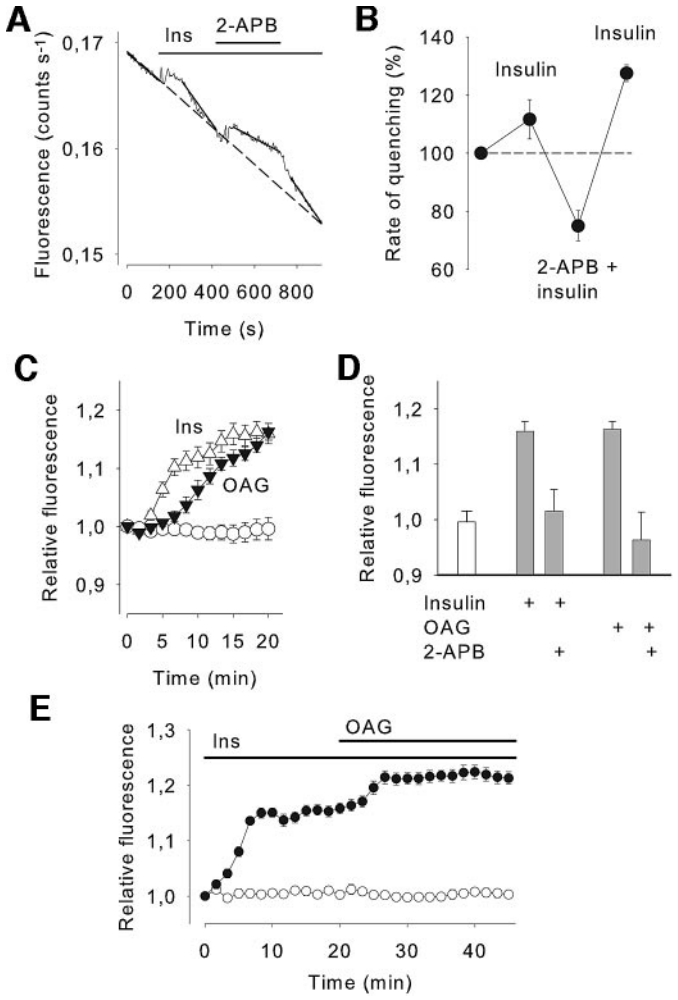


**FIG. 1.** ***A*****: Original records from a single skeletal muscle fiber during an $Mn^{2+}$-quenching experiment. Insulin and 2-APB (100 μmol/l) were added as indicated at the top. Straight lines represent linear fits used to measure the rate of quenching; dashed line shows the rate under basal conditions.** ***B*****: Mean data (±SE) from $Mn^{2+}$-quenching experiments ($n$ = 5). Data normalized to the rate of quenching before application of insulin.** ***C*****: Mean Calcium Green-1 fluorescence measurements during $Ba^{2+}$ (1 mmol/l) exposure. Insulin (△) or OAG (30 μmol/l; ▲) were applied at time 0 min; ○, $Ba^{2+}$ only. The fluorescence of each cell was normalized to the value at the start of exposure.** ***D*****: Relative Calcium Green-1 fluorescence at the end of 20-min exposures as indicated ($n$ ≥ 10 cells). □, $Ba^{2+}$ only.** ***E*****: Mean Calcium Green-1 fluorescence during $Ba^{2+}$ exposure with application of insulin followed by OAG as indicated (●; $n$ = 14); ○, $Ba^{2+}$ only.**

We also studied the combined effect of insulin plus OAG on $Ba^{2+}$ influx (Fig. 1*E*). When OAG was added in the continued presence of insulin, there was an ~40% additional increase in the signal as compared with the increase induced by insulin alone ($P < 0.001$). Noteworthy, the time to reach half of the maximum OAG-induced increase in the presence of insulin was ~5 min, which is markedly faster than when OAG was added on its own (~12 min).

**Effects of 2-APB on basal $Ca^{2+}$ influx.** Application of 2-APB caused a marked decrease of the rate $Mn^{2+}$ quenching under basal conditions (i.e., no insulin present) (Fig. 2*A*), and mean data show that 2-APB reduced the rate of quenching to ~30% of the control rate ($P < 0.001$) (Fig. 2*B*). Intriguingly, there was a marked increase in the rate of quenching when insulin was added in the presence of 2-APB. In fact, the effect of insulin on the rate of quenching was much larger in the presence than in the absence of 2-APB (Figs. 1 and 2). Nevertheless, in the presence of insulin plus 2-APB, the rate of quenching was decreased to 60–70% of the control rate with either insulin or 2-APB added first.

The effect of 2-APB on basal $Ca^{2+}$ influx was also tested with the $Ba^{2+}$ influx method. Measurements performed during the normal 20-min measuring period without adding $Ba^{2+}$ to the solution showed a significantly ($P < 0.05$) lower fluorescent signal (~0.9 of the control) than when $Ba^{2+}$ was added (~1.0 of the control) (Fig. 2*C*); this decrease in the Calcium Green-1 signal without $Ba^{2+}$ might represent leakage of the dye out of the cell, or some bleaching of the dye, due to repeated exposures to the laser light, which would be counteracted by influx of $Ba^{2+}$ when the ion was present. When $Ba^{2+}$ was added together with 2-APB, the fluorescent signal had decreased down to the level observed without $Ba^{2+}$ at the end of the 20-min exposure period (Fig. 2*C*). Thus, both the $Mn^{2+}$-quenching and the $Ba^{2+}$-influx experiments indicate that there is a basal $Ca^{2+}$ influx that can be inhibited by 2-APB.

**Glucose uptake in single FDB fibers.** Previous studies on isolated whole muscles have not shown any effect of decreasing bath [$Ca^{2+}$] on insulin-mediated glucose uptake (9,10). In accordance, we did not detect any effect on insulin-mediated 2-DG uptake in EDL muscles exposed to a Tyrode solution with 4 mmol/l EGTA and no $Ca^{2+}$ added (113.5 ± 4.8 vs. 103.5 ± 6.3 μmol/l per min in control; $n$ = 4). However, in a normally polarized skeletal muscle cell, the extracellular [$Ca^{2+}$] concentration has to be <1 nmol/l before the inward driving force for $Ca^{2+}$ is abolished, and in isolated FDB fibers, the bath [$Ca^{2+}$] has to be decreased to 1 nmol/l to significantly reduce the insulin-mediated increase in $[Ca^{2+}]_{mem}$ (14). Thus, it is doubtful whether the extracellular [$Ca^{2+}$] in isolated whole muscles can be decreased to levels low enough to affect insulin-induced $Ca^{2+}$ uptake and, hence, glucose transport. We therefore used fluorescent 2-DG (2-NBDG) to assess glucose uptake

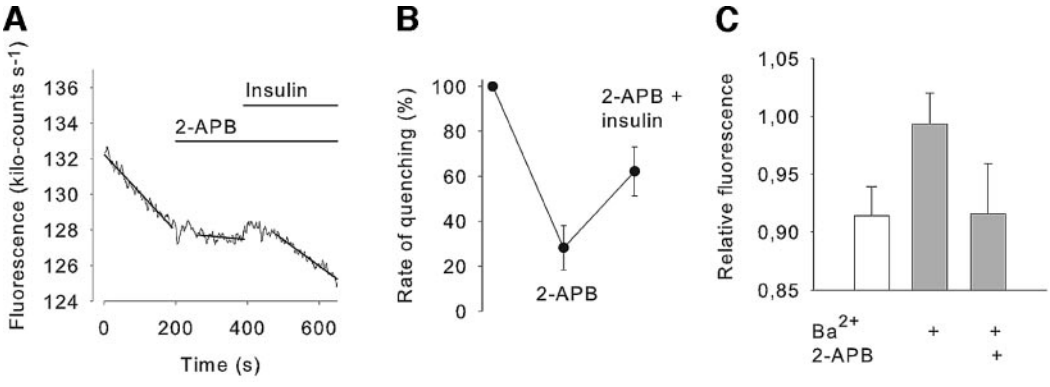


**FIG. 2.** ***A*****: Original records from an $Mn^{2+}$-quenching experiment. 2-APB (100 μmol/l) and insulin were added as indicated.** ***B*****: Mean data (±SE) from $Mn^{2+}$-quenching experiments ($n$ = 6).** ***C*****: Mean data of the relative Calcium Green-1 fluorescence at the end of 20-min exposures to $Ba^{2+}$ with or without 2-APB as indicated; □, no $Ba^{2+}$ added ($n$ ≥ 11 cells).**

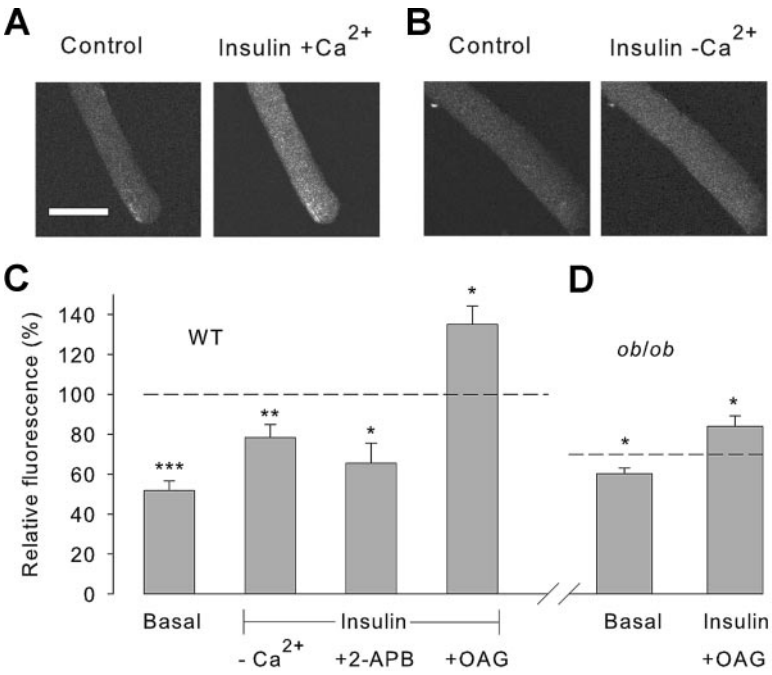


**FIG. 3. Confocal images of single muscle fibers exposed to 2-NBDG. Images obtained after exposure to 2-NBDG under control conditions, followed by exposure in the presence of insulin in normal [$Ca^{2+}$] (1.8 mmol/l) (*A*) and low [$Ca^{2+}$] (~1 nmol/l) (*B*). *C* and *D*: Mean data (±SE) of the relative 2-NBDG fluorescence under the indicated conditions compared with application of insulin alone (dashed lines), which was set to 100% in wild-type and to 70% in *ob/ob* mice (to adjust for insulin resistance) (28). Data obtained in cells from wild-type (*C*) and *ob/ob* (*D*) mice ($n \geq 9$ cells). *$P < 0.05$, **$P < 0.01$, and ***$P < 0.001$ vs. insulin in normal $Ca^{2+}$.**

in single FDB fibers. Under control conditions, $\Delta F_{c\text{-}b}/\Delta F_{b\text{-}a}$ after insulin (60 nmol/l) exposure (0.96 ± 0.08; $n = 27$) was about twice as large as that without insulin (0.50 ± 0.05; $n = 21$; $P < 0.001$), which demonstrates that the isolated cells respond to insulin with increased glucose uptake. The insulin-mediated increase in 2-NBDG fluorescence was markedly reduced when cells were exposed to low [$Ca^{2+}$] (~1 nmol/l) (Fig. 3*A* and *B*), and mean data show that ~40% of the normal insulin response was lost in low [$Ca^{2+}$] (Fig. 3*C*).

The application of 2-APB (100 μmol/l) significantly decreased the insulin-induced increase in 2-NBDG uptake by ~60% (Fig. 3*C*). Insulin plus OAG increased the $Ca^{2+}$ influx above that observed by insulin alone (Fig. 1*E*), which suggests that application of both agents would result in an increased glucose uptake. Accordingly, exposure to insulin plus OAG (30 μmol/l) gave a 2-NBDG fluorescence that was significantly larger than that of insulin alone (Fig. 3*C*). We also measured the 2-DG uptake in whole EDL muscles exposed to insulin plus OAG and found a significantly larger uptake (98.7 ± 5.7 μmol/l per min) compared with insulin alone (79.0 ± 3.0 μmol/l per min) ($P < 0.01$; $n = 8$).

The uptake of 2-NBDG was also tested in single FDB fibers of obese *ob/ob* mice. These mice are insulin resistant with an insulin-mediated 2-DG uptake in EDL muscles that is ~30% lower than in wild type (28). Accordingly, the insulin response in single *ob/ob* FDB fibers was small (Fig. 3*D*), and while insulin caused an approximate twofold increase in 2-NBDG uptake in wild-type cells, the increase was only ~1.2-fold in *ob/ob* fibers. Exposure to insulin plus OAG resulted in a significantly increased 2-NBDG uptake compared with insulin alone in *ob/ob* fibers as well.

**The effect of 2-APB and MDL on insulin-mediated glucose uptake in whole fast- and slow-twitch muscles.** Application of 2-APB resulted in a dose-dependent decrease in insulin-mediated 2-DG uptake in mouse fast-twitch EDL and slow-twitch soleus muscles (Fig. 4*A* and *B*). In whole FDB muscles, application of 2-APB (100 μmol/l) approximately halved the 2-DG uptake in the presence of insulin ($n = 4$, $P < 0.01$). The inhibitory effect of 2-APB on insulin-mediated 2-DG uptake was not restricted to mouse muscle, since similar results were obtained in rat EDL and soleus muscles (Fig. 4*C*). Thus, 100 μmol/l 2-APB decreased insulin-mediated 2-DG uptake by ~50% in fast- and slow-twitch muscles of mouse and rat. We also tested the effect of MDL, another inhibitor of nonselective cation channels that is structurally different to 2-APB (25). Application of MDL (100 μmol/l) resulted in a marked decrease in insulin-mediated 2-DG uptake in both EDL and soleus muscles ($P < 0.001$) (Fig. 4*D*).

Measurements of insulin-mediated 2-DG uptake were also performed in EDL muscles that had been exposed to 2-APB for 30 min and the drug then removed in the continued presence of insulin (i.e., a situation where $Ca^{2+}$ influx was markedly increased) (Fig. 1*B*). The results showed a significant (~30%; $P < 0.01$) increase in 2-DG uptake after 2-APB removal compared with insulin alone (Fig. 4*E*). To determine whether the insulin effect could also be potentiated in insulin-resistant muscles, we repeated the same experiment in EDL muscles from *ob/ob* mice. Indeed, the 2-APB rebound effect was also present in the insulin-resistant *ob/ob* muscles (~15% increase; $P < 0.05$) (Fig. 4*E*).

**The effect of 2-APB and OAG on basal, hypoxia-, and contraction-mediated glucose uptake in whole muscles.** Basal 2-DG uptake in EDL and soleus muscles was not significantly affected by 2-APB, MDL, or OAG (Fig. 5*A*). Hypoxia or repeated contractions are known to increase glucose uptake in skeletal muscle by pathways that differ from that of insulin (29). Hypoxia (induced by exposing muscles to $N_2$) resulted in about a twofold increase in 2-DG uptake that was not affected by 2-APB or OAG (Fig. 5*B*). Repeated tetanic contractions for 10 min increased 2-DG uptake about threefold in EDL muscles, and this increase was not affected by 2-APB or OAG (Fig. 5*C*). We added 2-APB or OAG after the series of contractions because skeletal muscles have been shown to take up $Ca^{2+}$ during repeated contractions (30), and we wanted to avoid potential problems with differences in sarcolemmal $Ca^{2+}$ fluxes during the contraction period. It might then be argued that 2-APB and OAG can only exert their effects if

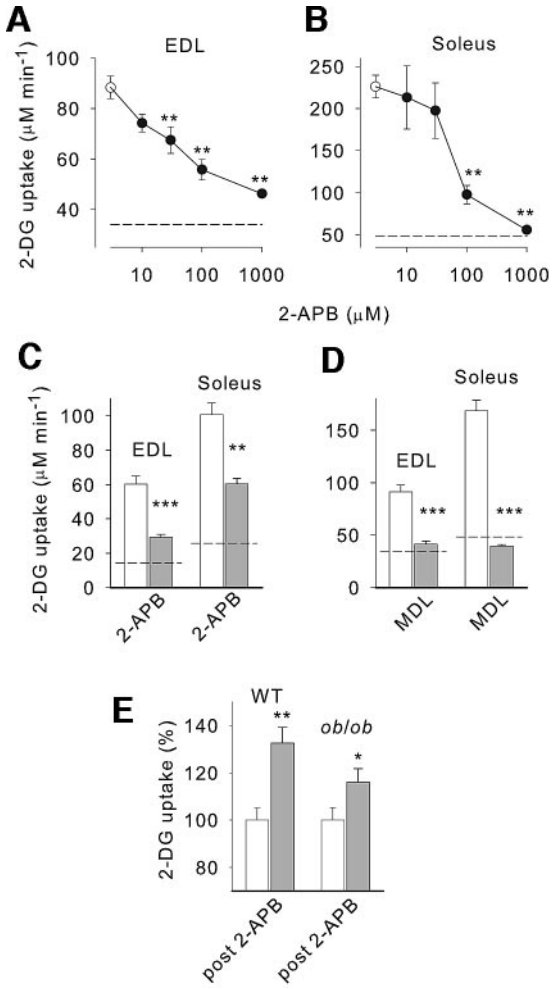


**FIG. 4. Measurements of insulin-mediated 2-DG uptake in isolated whole muscles. The effect of 2-APB in mouse EDL (*A*) and soleus (*B*) muscles ($n$ = 4–11). *C*: The response to 100 μmol/l 2-APB in rat muscles ($n$ = 6). *D*: The effect of 100 μmol/l MDL in mouse muscles ($n$ = 4–6). Data are presented as means ± SE. Open and filled circles/bars represent insulin (120 nmol/l) only and in the presence of inhibitor, respectively. Dashed lines indicate 2-DG uptake under basal conditions (no insulin). *E*: Removal of 2-APB in the continued presence of insulin resulted in increased 2-DG uptake in both wild-type ($n$ = 8) and *ob/ob* ($n$ = 15) EDL muscles (■). The mean uptake with insulin only was set to 100% (□). *$P$ < 0.05, **$P$ < 0.01, and ***$P$ < 0.001 vs. insulin alone.**

they are present during the induction of increased glucose uptake. However, control experiments, in which EDL and soleus muscles were exposed to insulin for 30 min before adding 2-APB (100 μmol/l) and measuring 2-DG uptake, showed ~35% lower uptake in the presence than in the absence of 2-APB ($P < 0.001$). Thus, while 2-APB and OAG significantly affected insulin-mediated $Ca^{2+}$ fluxes and glucose uptake, they had no significant effect on other modes of glucose uptake.

**The effect of 2-APB on tetanic force and $[Ca^{2+}]_i$.** Tetanic force and $[Ca^{2+}]_i$ were measured in isolated FDB fibers before and immediately after or during exposure to 2-APB. Records of tetanic $[Ca^{2+}]_i$ from a representative experiment are shown in Fig. 5*D*. Mean data showed that tetanic force was 100 ± 5% and $[Ca^{2+}]_i$ 99 ± 10% of that before 2-APB exposure ($n$ = 6). Tetanic force was also measured in whole muscles exposed to 2-APB (100 μmol/l). After 30 min exposure, tetanic force was increased by 14 ± 4% in soleus ($n$ = 5, $P < 0.05$) and 7 ± 5% in EDL muscles ($n$ = 4, $P > 0.05$) and the relaxation speed slightly decreased. Thus, 2-APB had no adverse effect on action potential–mediated sarcoplasmic reticulum $Ca^{2+}$ release and force production.

**The effect of 2-APB on intracellular insulin signaling.** Insulin increased PKB (Akt) phosphorylation, and this increase was not affected by 2-APB (Fig. 6*A*). The insulin-induced phosphorylation of PKB was absent in the presence of wortmannin (0.5 μmol/l), which inhibits phosphoinositide 3-kinase; this phosphorylation is an early step in the insulin signaling cascade (4). 2-APB and wortmannin, on their own, had no effect on PKB phosphorylation, nor did any of the treatments significantly affect the total PKB expression (data not shown). Insulin significantly ($P < 0.05$) increased ERK1/2 phosphorylation in both the absence and presence of 2-APB (Fig. 6*B*). These findings demonstrate that 2-APB interferes neither with early signaling steps in the pathway terminating with glucose uptake nor with the branch of the insulin signaling cascade that results in mitogen-activated protein kinase activation (31).

## DISCUSSION

The present study shows that changes in $Ca^{2+}$ influx have significant effects on insulin-mediated glucose uptake in skeletal muscle. By manipulating the $Ca^{2+}$ influx, we could both decrease (in the presence of 2-APB, MDL, or low extracellular $[Ca^{2+}]$) and increase (after removal of 2-APB or in the presence of OAG) the insulin response. On the other hand, a solitary change in the $Ca^{2+}$ influx is not enough to alter glucose transport because decreased (with 2-APB) or increased (with OAG) $Ca^{2+}$ influx had no effect on 2-DG uptake in the absence of insulin. This means that insulin activates additional factors that are required for stimulation of glucose uptake. The insulin-induced activation of these additional factors is probably mediated via the PKB/Akt and/or CAP-cbl-TC10 pathways (2,3), because 2-APB and OAG had no effect on hypoxia- or contraction-mediated glucose uptake, which are mediated via signaling pathways different from those of insulin (29).

The present results show a complex interaction between basal, insulin- and OAG-mediated $Ca^{2+}$ influx (Figs. 1 and 2), which indicates the involvement of several different ion channels or a complex regulation of one set of channels. Earlier studies suggested the involvement of voltage-activated L-type $Ca^{2+}$ channels in insulin action because pharmacological inhibition of these channels reduced insulin-mediated increases in glucose uptake in rat muscle (32) and $[Ca^{2+}]_{mem}$ in mouse FDB fibers (14). However, L-type $Ca^{2+}$ channels are normally activated upon depolarization, and insulin causes a hyperpolarization of the sarcolemma (14,33). Also, there was no simple relationship between $Ca^{2+}$ uptake and glucose transport in the presence of $Ca^{2+}$ channel blockers (32). Thus, the present results show an important modulating role of $Ca^{2+}$ influx in insulin-mediated glucose uptake, but the identity of the ion channels involved remains uncertain.

The changes in $Ca^{2+}$ influx induced by insulin, 2-APB, and OAG were rather small and would have limited effect on $[Ca^{2+}]_i$ (14,15), but still, they had a major impact on insulin-mediated glucose uptake. This implicates a model with strict spatial control of these $Ca^{2+}$ fluxes with participating $Ca^{2+}$ channels being located in close vicinity to other components required for glucose transport. The situation would resemble that in neurons where the diverse response to activation of different $Ca^{2+}$ channels

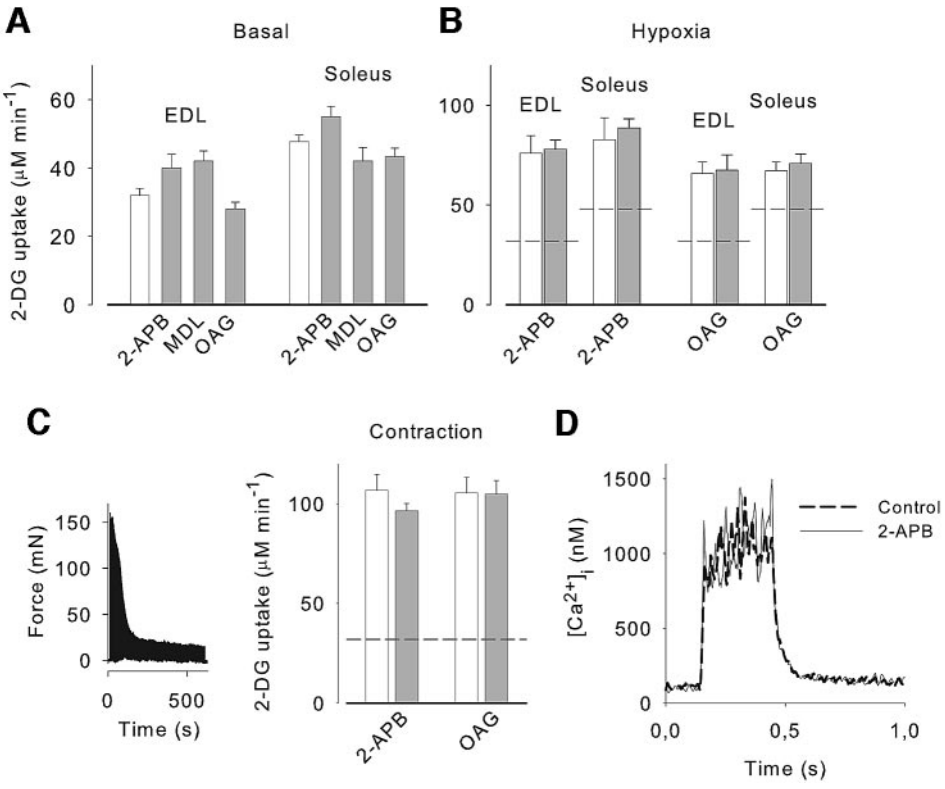


**FIG. 5. Mean data (±SE) of basal (*A*) ($n \geq 4$), hypoxia-mediated (*B*) ($n = 5–6$), and contraction-mediated (*C*) ($n = 5–6$) 2-DG uptake. □, control conditions; ■, in the presence of the drug indicated (2-APB and MDL 100 μmol/l; OAG 30 μmol/l). *Left panel* in *C* shows a representative force record from repeated contractions produced to induce contraction-mediated glucose uptake. Dashed lines in *B* and *C* indicate 2-DG uptake under basal conditions. *D*: Original $[Ca^{2+}]_i$ records from tetanic contractions (70 Hz, 350 ms) of an isolated FDB fiber before (Control) and after application of 2-APB (100 μmol/l).**

seems to be caused by physically associated signaling molecules that sense local $Ca^{2+}$ increases at the mouth of the channels (34). The $Ca^{2+}$-binding protein calmodulin has a central role in this process (35). Interestingly, pharmacological inhibition of calmodulin/calmodulin kinase decreases insulin-mediated glucose uptake (24,36).

$Ca^{2+}$ influx appears to act on later steps in the insulin signaling pathway, since 2-APB did not affect PKB or ERK1/2 phosphorylation (Fig. 6). Several steps in the docking and fusion of GLUT4 transporters into the plasma membrane are potentially $Ca^{2+}$/calmodulin sensitive (37); in other words, this process may be similar to the $Ca^{2+}$-dependent docking of synaptic vesicles in nerve terminals (38). Furthermore, results from an in vitro assay for GLUT-4 translocation show that the association of GLUT-4 with the plasma membrane is $Ca^{2+}$ dependent (39).

In conclusion, $Ca^{2+}$ influx is an important modulator of insulin-mediated glucose uptake. The present results indicate that therapeutic interventions that increase $Ca^{2+}$ influx in association with insulin exposure may be used to improve glucose uptake in insulin-resistant conditions. As a proof of principle, we show that increased $Ca^{2+}$ influx is accompanied by increased insulin-mediated glucose uptake in insulin-resistant muscles.

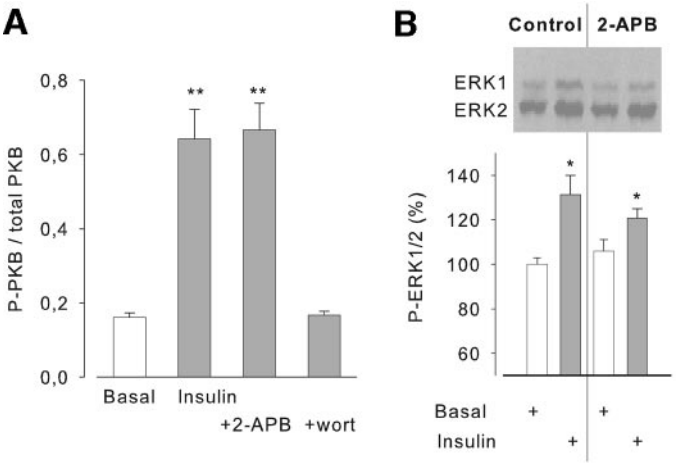


**FIG. 6. *A*: Mean data (±SE) from enzyme-linked immunosorbent assay analysis of the proportion of phosphorylated to total PKB under basal conditions (□) and in the presence of insulin with or without 2-APB (100 μmol/l) or wortmannin (0.5 μmol/l) (■). *B*: Representative immunoblots of phosphorylated mitogen-activated protein kinase ERK1/2 in EDL muscles exposed to insulin with or without 2-APB. *Lower panel* shows mean data ($n = 5$) normalized to the mean basal control value, which was set to 100%. *$P < 0.05$ and **$P < 0.01$ vs. basal control.**

## ACKNOWLEDGMENTS

This study was supported by the Swedish Research Council, the Biovitrum Partner Fund, the Swedish Diabetes Foundation, the Swedish National Center for Sports Research, and funds at the Karolinska Institutet.

## REFERENCES

1. DeFronzo RA, Gunnarsson R, Björkman O, Olsson M, Wahren J: Effects of insulin on peripheral and splanchnic glucose metabolism in noninsulin-dependent (type II) diabetes mellitus. *J Clin Invest* 76:149–155, 1985
2. Khan AH, Pessin JE: Insulin regulation of glucose uptake: a complex interplay of intracellular signalling pathways. *Diabetologia* 45:1475–1483, 2002
3. Bryant NJ, Govers R, James DE: Regulated transport of the glucose transporter GLUT4. *Nat Rev Mol Cell Biol* 3:267–277, 2002
4. White MF: Insulin signaling in health and disease. *Science* 302:1710–1711, 2003
5. Schudt C, Gaertner U, Pette D: Insulin action on glucose transport and calcium fluxes in developing muscle cells in vitro. *Eur J Biochem* 68:103–111, 1976
6. Clausen T: The role of calcium in the activation of the glucose transport system. *Cell Calcium* 1:311–325, 1980
7. Bihler I, Charles P, Sawh PC: Effects of strontium on calcium-dependent hexose transport in muscle. *Can J Physiol Pharmacol* 64:176–179, 1986

8. Westfall MV, Sayeed MM: Effect of $Ca^{2+}$-channel agonists and antagonists on skeletal muscle sugar transport. *Am J Physiol* 258:R462–R468, 1990
9. Wallberg-Henriksson H, Campaigne BN, Henriksson J: In vitro reversal of insulin resistance in diabetic skeletal muscle is independent of extracellular $Ca^{2+}$ and $Mg^{2+}$. *Acta Physiol Scand* 133:125–126, 1988
10. Henriksen EJ, Rodnick KJ, Holloszy JO: Activation of glucose transport in skeletal muscle by phospholipase C and phorbol ester: evaluation of the regulatory roles of protein kinase C and calcium. *J Biol Chem* 264:21536–21543, 1989
11. Klip A, Ramlal T: Cytoplasmic $Ca^{2+}$ during differentiation of 3T3–L1 adipocytes: effect of insulin and relation to glucose transport. *J Biol Chem* 262:9141–9146, 1987
12. Cheung JY, Constantine JM, Bonventre JV: Cytosolic free calcium concentration and glucose transport in isolated cardiac myocytes. *Am J Physiol* 252:C163–C172, 1987
13. Klip A, Li G, Logan WJ: Role of calcium ions in insulin action on hexose transport in L6 muscle cells. *Am J Physiol* 247:E297–E304, 1984
14. Bruton JD, Katz A, Westerblad H: Insulin increases near-membrane but not global $Ca^{2+}$ in isolated skeletal muscle. *Proc Natl Acad Sci U S A* 96:3281–3286, 1999
15. Bruton JD, Katz A, Westerblad H: The role of $Ca^{2+}$ and calmodulin in insulin signalling in mammalian skeletal muscle. *Acta Physiol Scand* 171:259–265, 2001
16. Bootman MD, Collins TJ, Mackenzie L, Roderick HL, Berridge MJ, Peppiatt CM: 2-aminoethoxydiphenyl borate (2-APB) is a reliable blocker of store-operated $Ca^{2+}$ entry but an inconsistent inhibitor of InsP3-induced $Ca^{2+}$ release. *FASEB J* 16:1145–1150, 2002
17. Trebak M, Bird GS, McKay RR, Putney JW: Comparison of human TRPC3 channels in receptor-activated and store-operated modes: differential sensitivity to channel blockers suggests fundamental differences in channel composition. *J Biol Chem* 277:21617–21623, 2002
18. Lievremont JP, Bird GS, Putney JW Jr: Mechanism of inhibition of TRPC cation channels by 2-aminoethoxydiphenylborane. *Mol Pharmacol* 68:758–762, 2005
19. Hofmann T, Obukhov AG, Schaefer M, Harteneck C, Gudermann T, Schultz G: Direct activation of human TRPC6 and TRPC3 channels by diacylglycerol. *Nature* 397:259–263, 1999
20. Lännergren J, Westerblad H: The temperature dependence of isometric contractions of single, intact fibres dissected from a mouse foot muscle. *J Physiol* 390:285–293, 1987
21. Liu Y, Kranias EG, Schneider MF: Regulation of $Ca^{2+}$ handling by phosphorylation status in mouse fast- and slow-twitch skeletal muscle fibers. *Am J Physiol* 273:C1915–C1924, 1997
22. Hopf FW, Reddy P, Hong J, Steinhardt RA: A capacitative calcium current in cultured skeletal muscle cells is mediated by the calcium-specific leak channel and inhibited by dihydropyridine compounds. *J Biol Chem* 271:22358–22367, 1996
23. Lloyd PG, Hardin CD, Sturek M: Examining glucose transport in single vascular smooth muscle cells with a fluorescent glucose analog. *Physiol Res* 48:401–410, 1999
24. Shashkin P, Koshkin A, Langley D, Ren JM, Westerblad H, Katz A: Effects of CGS 9343B (a putative calmodulin antagonist) on isolated skeletal muscle: dissociation of signaling pathways for insulin-mediated activation of glycogen synthase and hexose transport. *J Biol Chem* 270:25613–25618, 1995
25. van Rossum DB, Patterson RL, Ma HT, Gill DL: $Ca^{2+}$ entry mediated by store depletion, S-nitrosylation, and TRP3 channels. *J Biol Chem* 275:28562–28568, 2000
26. Sandström ME, Abbate F, Andersson DC, Zhang SJ, Westerblad H, Katz A: Insulin-independent glycogen supercompensation in isolated mouse skeletal muscle: role of phosphorylase inactivation. *Pflugers Arch* 448:533–538, 2004
27. Wretman C, Lionikas A, Widegren U, Lännergren J, Westerblad H, Henriksson J: Effects of concentric and eccentric contractions on phosphorylation of $MAPK^{erk1/2}$ and $MAPK^{p38}$ in isolated rat skeletal muscle. *J Physiol* 535:155–164, 2001
28. Fauconnier J, Lanner JT, Zhang SJ, Tavi P, Bruton JD, Katz A, Westerblad H: Insulin and inositol 1,4,5-trisphosphate trigger abnormal cytosolic $Ca^{2+}$ transients and reveal mitochondrial $Ca^{2+}$ handling defects in cardiomyocytes of *ob/ob* mice. *Diabetes* 54:2375–2381, 2005
29. Nolte LA, Han DH, Hansen PA, Hucker KA, Holloszy JO: A peroxovanadium compound stimulates muscle glucose transport as powerfully as insulin and contractions combined. *Diabetes* 52:1918–1925, 2003
30. Mikkelsen UR, Fredsted A, Gissel H, Clausen T: Excitation-induced $Ca^{2+}$ influx and muscle damage in the rat: loss of membrane integrity and impaired force recovery. *J Physiol* 559:271–285, 2004
31. Saltiel AR, Kahn CR: Insulin signalling and the regulation of glucose and lipid metabolism. *Nature* 414:799–806, 2001
32. Cartee GD, Briggs-Tung C, Holloszy JO: Diverse effects of calcium channel blockers on skeletal muscle glucose transport. *Am J Physiol* 263:R70–R75, 1992
33. Clausen T, Flatman JA: Effects of insulin and epinephrine on $Na^+$-$K^+$ and glucose transport in soleus muscle. *Am J Physiol* 252:E492–E499, 1987
34. West AE, Chen WG, Dalva MB, Dolmetsch RE, Kornhauser JM, Shaywitz AJ, Takasu MA, Tao X, Greenberg ME: Calcium regulation of neuronal gene expression. *Proc Natl Acad Sci U S A* 98:11024–11031, 2001
35. Mori MX, Erickson MG, Yue DT: Functional stoichiometry and local enrichment of calmodulin interacting with $Ca^{2+}$ channels. *Science* 304:432–435, 2004
36. Brozinick JT Jr, Reynolds TH, Dean D, Cartee G, Cushman SW: 1-[*N*,*O*-Bis-(5-isoquinolinesulphonyl)-*N*-methyl-L-tyrosyl]-4-phenylpiperazine (KN-62), an inhibitor of calcium-dependent camodulin protein kinase II, inhibits both insulin- and hypoxia-stimulated glucose transport in skeletal muscle. *Biochem J* 339:533–540, 1999
37. Whitehead JP, Molero JC, Clark S, Martin S, Meneilly G, James DE: The role of $Ca^{2+}$ in insulin-stimulated glucose transport in 3T3–L1 cells. *J Biol Chem* 276:27816–27824, 2001
38. Zenisek D, Steyer JA, Almers W: Transport, capture and exocytosis of single synaptic vesicles at active zones. *Nature* 406:849–854, 2000
39. Inoue G, Cheatham B, Kahn CR: Development of an in vitro reconstitution assay for glucose transporter 4 translocation. *Proc Natl Acad Sci U S A* 96:14919–14924, 1999